Applied Catalysis B: Environmental 179 (2015) 88–94

Contents lists available at ScienceDirect

Applied Catalysis B: Environmental

journal homepage: www.elsevier.com/locate/apcatb

Kinetics of hydrogen evolution reaction in alkaline electrolysis on a Ni cathode in the presence of Ni–Co–Mo based ionic activators

Vladimir M. Nikolic[a,*], Sladjana Lj. Maslovara[a], Gvozden S. Tasic[a], Tanja P. Brdaric[a], Petar Z. Lausevic[a,b], Bojan B. Radak[a], Milica P. Marceta Kaninski[a]

[a] University of Belgrade, Vinča Institute of Nuclear Sciences, Department of Physical Chemistry, 11001 Belgrade, Serbia
[b] School of Electrical Enginering, University of Belgrade, Serbia

ARTICLE INFO

Article history:
Received 14 February 2015
Received in revised form 2 May 2015
Accepted 6 May 2015
Available online 7 May 2015

Keywords:
Hydrogen evolution reactionl
In-situ activation
Ionic activator
Alkaline electrolyzer

ABSTRACT

This paper presents investigations on the influence of *in-situ* ionic activation using combination of three D-metals: Ni, Co and Mo on the hydrogen evolution reaction (HER) mechanism and kinetics. Polarization measurements were performed to obtain kinetic parameters for the HER and the results are presented to show Tafel slopes, exchange current densities and apparent energy of activation. The values of the kinetic parameters confirm the existence of two Tafel slopes, in the case of NiCoMo based ionic activators (i.a.) in the investigated temperature range, with very high values of the exchange current density. Electrochemical impedance spectroscopy measurements were employed to further investigate the origin of the obtained electrocatalytic effect on the HER. The measurements were performed at several overpotentials and temperatures. It was found that co-deposition of Ni, Co and Mo species on the Ni cathode results in a large number of active sites for hydrogen adsorption, and a synergetic effect giving electronic structure suitable for the HER, are the main factors contributing to the enhanced HER kinetics. It was shown that EIS measurements had a crucial role in determining the HER mechanism, especially with the complex *in-situ* activation of the alkaline electrolysis.

1. Introduction

Because of the rapidly increasing energy demands more attention has to be paid to renewable and clean energy sources. Hydrogen is considered to be the main medium for energy storage in the future since the energy can be stored in the form of chemical energy and transformed into electrical energy in fuel cells. There are very promising prospects for the large-scale production of hydrogen from wind, water and solar energy in the future, and, it will be a key strategy for energy storage. The use of hydrogen in fuel cells does not cause pollution of the environment, as the only by-product is water. One of the most commonly used technologies for hydrogen production is alkaline electrolysis [1,2]. The alkaline water electrolysis is a well known techonological process, which essentially takes in pure water and DC electricity and outputs H_2 and O_2. Commercial alkaline water electrolysers utilize stainless steel, Ni or Raney Ni as cathode, and operate with potassium hydroxide solution in the concentration range 6–9 mol/l and in the temperature range 60–80 °C [3].

Good electrode materials for alkaline electrolysers should exhibit: high electrical conductivity, high corrosion resistance and minimum overvoltage. The main issue with commercial cathodes is the decrease of their electrochemical activity over time [4,5]. One promising aproach which enables to avoid such losses and to enhance the efficiency of the electrolyser is the addition of catalysts in the supporting electrolyte (*in-situ* activation) [6,7]. *In-situ* activation is achieved by direct dissolution of the activating compounds in the electrolyte during the electrolytic process. *In-situ* activation does not require a separate surface activation step which adds considerably to the cost of the cathode. According, to Brewer hypo-hyper-D-interionic bonding theory, suitable compounds for *in-situ* activation are systems that combine early transition with late transition D-electronic metals, since their bimetallic surfaces are expected to exhibit modified chemical properties compared to pure metal surfaces [8,9]. The increase of electrocatalytic activity has been explained by the synergetic electronic effect [10].

In our previous studies, we have investigated the electrocatalytic activity for the HER of several combinations of two D-metals added *in situ* in 6 M KOH solution. It was shown that ionic activa-

* Corresponding author. Tel.: +381 113408534; fax: +381 112447207.
E-mail address: nikolicv@vinca.rs (V.M. Nikolic).

http://dx.doi.org/10.1016/j.apcatb.2015.05.012
0926-3373/

tion using Ni–Mo and Co–Mo based ionic activator (i.a.), as well as ternary Ni–Co–Mo based i.a. resulted in significant increase of the HER efficiency and lowered energy consumption of the alkaline electrolyzer compared to standard, 6 M KOH electrolyte [7,11,12]. The aim of this work is to determine the influence of the Ni–Co–Mo based i.a. added *in situ* to the standard electrolyte, on the HER mechanism and kinetics. Polarization measurements were performed to obtain kinetics parameters for the HER and the results are presented to show Tafel slopes, exchange current densities and apparent energy of activation. Electrochemical impedance spectroscopy (EIS) was used to further explain the HER mechanism, as measurements were performed at several overpotentials and temperatures. The obtained spectra were fitted in order to determine the specific resistances and capacitances and the results were correlated to the parameters obtained from Tafel analysis.

2. Experimental

All measurements were performed in 6 M KOH solution (Merck) prepared in deionized water. As ionic activators, we used a mixture of three component: tris(ethylendiamine)Ni(II) chloride($[Ni(en)_3]Cl_2$), tris(ethylendiamine) Co(III) chloride ($[Co(en)_3]Cl_3$) synthesized from p.a. chemicals, and sodium molybdate (Na_2MoO_4) (Merck). The concentrations of Ni complex, Mo salt and Co complex were: 5×10^{-3} M, 1×10^{-2} M and 5×10^{-3} M, as this composition of the i.a. has shown the largest decrease in the energy consumption of alkaline electrolyzer [11].

All measurements were performed in standards three-compartment cell. The cell consisted of a large area platinum mesh (5 cm diameter and 5 cm height) as counter electrode, nickel (99.95% purity) as working electrode and Hg/HgO in 6 M KOH, as reference electrode. The latter was connected to the working electrode via Luggin capillary positioned close to the working electrode. The working electrode was a nickel plate with surface area of 2 cm^2. Before each experiment the nickel surface was first treated by etching in solution of nitric acid (concentration ratio HNO_3:H_2O = 2:1) for 2 min and then washed with distilled water. The inactive sides of the working electrode were protected from the solution by the alkaline resistant epoxy resin. The electrolyte in the working electrode compartment was purged with gaseous hydrogen during measurements.

The polarization diagrams were recorded by varying the temperature between 298 and 343 K using an ultrathermostat. Tafel curves were recorded by scaning the working electrode potential from −1.3 V to −0.8 V *vs.* Hg|HgO at the scan rate of 1 mV s^{-1}, using Gamry 750 G Potentiostat/Galvanostat/ZRE. Alternating current(AC) impedance spectra were recorded in the frequency range from 100 kHz to 100 mHz using 10 mV AC amplitude at the constant overpotentials in the range from −20 mV to −200 mV. Before each measurement the electrolyte solution in the cell was deoxygenated with hydrogen by continuous bubbling for 30 min.

3. Results and discussion

The determination of the reaction mechanism of the HER and the process rate determining step (RDS) can be accomplished using Tafel analysis. Generally, the overall reaction in alkaline solution proceeds via three steps reaction mechanism [13]:

$$M + H_2O + e^- \leftrightarrow MH_{ads} + OH^- \text{Volmer reaction} \quad (1)$$

$$MH_{ads} + H_2O + e^- \leftrightarrow H_2 + M + OH^- \text{Heyrovsky reaction} \quad (2)$$

$$MH_{ads} + MH_{ads} \leftrightarrow H_2 + M \text{ Tafel reaction} \quad (3)$$

The HER starts with proton discharge electrosorption step, Volmer reaction, followed by electronic-desorption step, Heyrovsky reaction and/or catalytic-recombination step, Tafel reaction. Thus, the overall reaction proceeds via two possible reaction pathways, Volmer–Heyrovsky and Volmer–Tafel. For each step (1)–(3) being RDS the Tafel slope has value of −120 mV dec^{-1}, −40 mV dec^{-1}, and −30 mV dec^{-1}, respectively.

Table 1
Kinetic parameters derived from Tafel analysis of the NiCoMo based i.a. system.

t (°C)	j_0 (A cm^{-2})	b_1 (mV dec^{-1})	b_2 (mV dec^{-1})
25	3.558 e-4	42.9	88.9
30	1.030 e-3	41.1	99.4
40	1.535 e-3	41.3	122.9
50	2.656 e-3	42.5	128.5
60	3.957 e-3	42.3	133.6
70	4.301 e-3	42.0	143.0

Fig. 1 presents polarization curves obtained for the *in-situ* activated electrolytic process in the temperature range 25–70 °C.

The kinetic parameters for the HER (j_o and b) for the investigated systems were derived from Tafel equation:

$$\eta = a + b \times \log j \quad (4)$$

where η (V) represents the applied overpotential, j (mA cm^{-2}) the resulting current density, b (V dec^{-1}) the Tafel slope and a (V) the intercept. This intercept is related to the exchange current density j_o, through equation:

$$a = \frac{(2.3RT)}{(\beta nF)} \times \log j_0 \quad (5)$$

$$b = \frac{2.3RT}{\beta nF} \quad (6)$$

where R is the gas constant (8.314 kJ mol^{-1} K^{-1}), β is the symmetry factor, n is the number of electrons exchanged and F is the Faraday constant (96,485 °C mol^{-1}). The results are presented in Table 1.

The polarization curves shown in Fig. 1(a) exhibit the expected behaviour with increasing operation temperatures; there is an evident increase of the exchange current denstiy and a slight decrease of the equilibrium potential. It is interesting to notice the deformation of the curves starting at lower overpotentials with increasing temperature, which suggests possible change in the HER mechanism. Fig. 1(b) shows comparison of the Tafel curves for 6 M KOH and 6 M KOH with NiCoMo based i.a. Comparison was made at 70 °C, since we have previously showed that the greatest decrease of the energy consumption of the alkaline electrolyzer occurs at this temperature [11]. The polarisation curve in the case of NiCoMo activated electrolyte shows the existence of two slopes: 42 mV dec^{-1} at lower potentials and 143 mV dec^{-1} at higher potentials. These findings suggest the Volmer–Heyrovsky reaction path for the HER, as in the case of standard electrolyte [12]. Following the results of the Tafel analysis the rate determining step (RDS) at low overvoltages is the Heyrovsky reaction, which is associated with the electro-desorption step. At higher overvoltages, the Volmer reaction is the RDS, as the charge transfer process determines the HER kinetics. This behaviour is in good agreement with the previously reported mechanism for the HER in 6 M KOH on a Ni based cathode [13]. The values of the kinetics parameters from Table 1 confirms the exsistance of two Tafel slopes, in the case of NiCoMo based i.a., with very high values of the exchange current density. These values of the exchange current density could be possibly explained with the expected increase of the cathode surface area, due to electrodeposition of ionic species from the NiCoMo based i.a. This electrodeposition process takes place simultaneously with hydrogen evolution, during the certain time period [11,12]. On the other hand, the existance of two Tafel slopes could be associated with the relation between the exchange current density and the electronic structure of the composite electrodeposits [14]. These observations

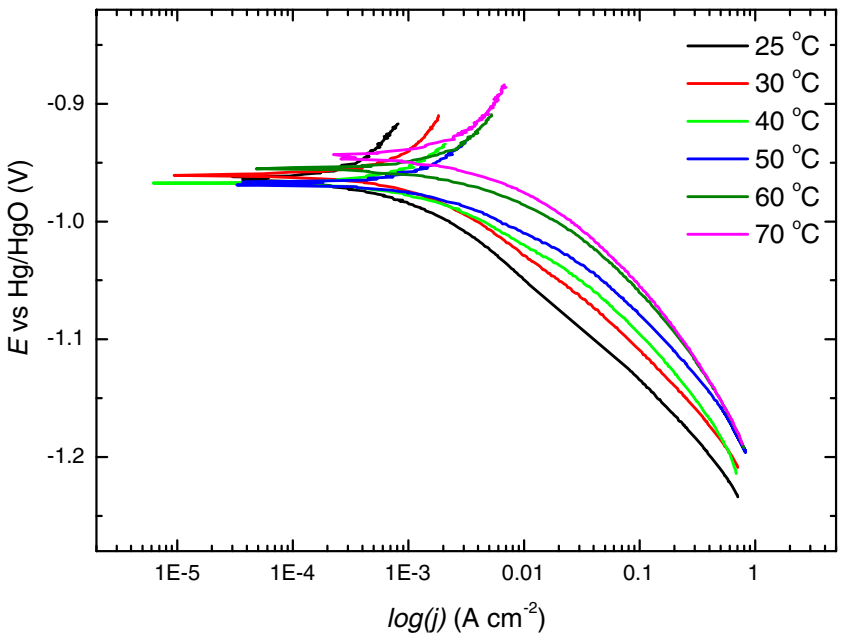

a)

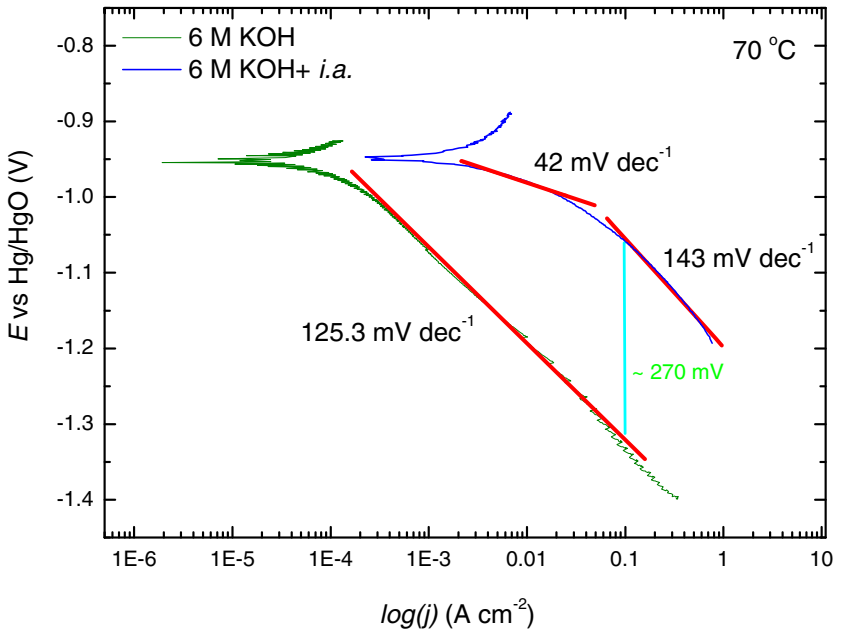

b)

Fig. 1. (a) Tafel curves obtained at Ni cathode with added NiCoMo based i.a. at different temperatures, (b) comparison of the Tafel curves for standard and *in situ* activated electrolyte at 70 °C.

could be explained through combining several effects. First, a synergetic effect of D-metals according to Brewer's theory which could exist because of the deposition of the D-metals from two branches of the Volcano curve [15]. Second, the facilitated hydride formation for Ni-Moalloying [16] and Rowland like effect of ethylenediamine, or trimethylenediamine ligands present in the activated electrolyte [17].

There is another important aspect shown in Fig. 1(b), when comparing the polarisation behaviour of the nickel cathode in standard and *in-situ* activated electrolyte. At fixed current density value, 0.1 A cm^{-2}, there is significant decrease in the HER overvoltage of about 270 mV. This finding is very important since these operating conditions (70 °C and 0.1 A cm^{-2}) are close to the operating conditions of the commercial alkaline electrolyzers.

In order to determine the origin of the observed change in the HER mechanism, EIS measurements were performed for both, 6 M KOH and 6 M KOH + NiCoMo based i.a., at different overvoltages at room temperature, Fig. 2.

The EIS spectra presented in Fig. 2 exhibit the expected behavior when increasing cathodic overvoltage at room temperature, i.e. the total resistance is decreasing with increasing HER overvoltage. The shape of the Nyquist plots is represented with single

Table 2
Comparison of EIS parameters for standard 6 M KOH electrolyte at 298 K and NiCoMo based i.a. at different temperatures, at a cathodic overvoltage of 150 mV.

T(K)	Electrolyte	R_e (Ω cm^2)	R_{ct} (Ω cm^2)	C_{dl} (F cm^{-2})	C_p (F cm^{-2})	R_p (Ω cm^2)	σ
298	6M KOH	0.365	400.9	1.820 e-4	–	–	9.1
298	6M	0.473	2.63	1.480 e-2	1.878 e-3	0.226	740
303	KOH	0.457	2.224	3.543 e-2	1.152 e-3	0.566	1771
313	+	0.393	1.841	1.054 e-1	4.212 e-4	0.718	5270
323	NiCoMo	0.274	0.903	8.797 e-2	3.373 e-3	1.016	4398
333		0.317	0.71	1.777 e-1	4.204 e-4	0.772	8885
343		0.274	0.467	1.825 e-1	1.325 e-4	0.962	9124

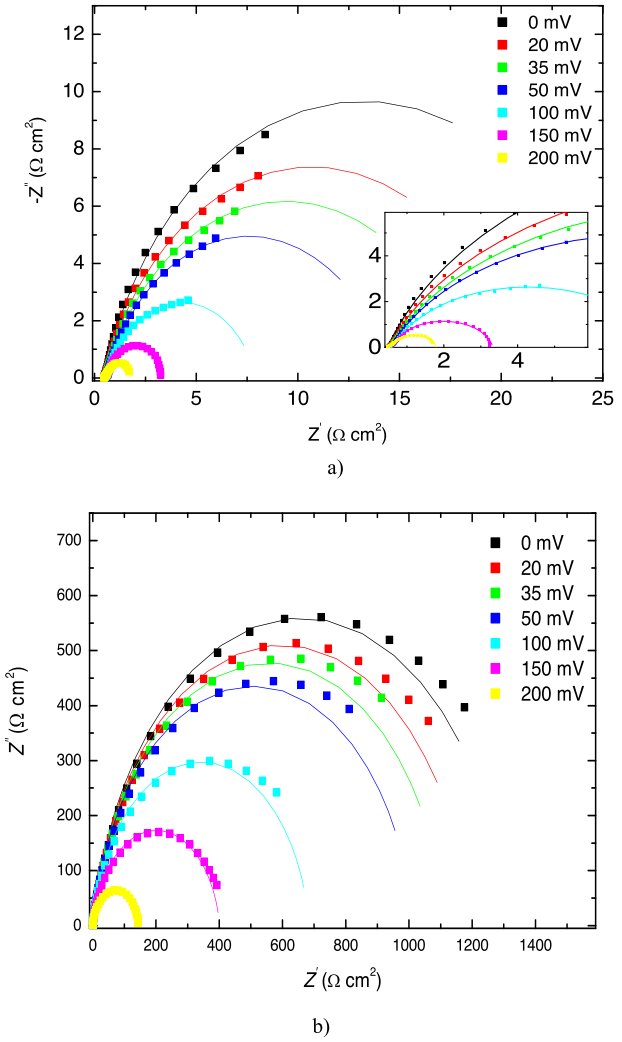

Fig. 2. Nyquist plots for (a) NiCoMo based i.a. insert represent high frequency region, and (b) standard electrolyte at increased cathodic overvoltage at 298 K. The lines were are obtained by fitting procedure using Randles equivalent circuit.

semicircle, however when comparing the Nyquist plots for NiCoMo based i.a. and standard electrolyte, it can be seen there is an appearance of a second smaller semicircle in the high frequency region at higher overvoltages. Also, it is noticable that the total resistance of the nickel cathode in standard electrolyte is about two orders of magnitude higher than that for the electrolyte with NiCoMo based i.a.

Nyquist plots presented at Fig. 3 were obtained by measuring the frequency response of the cathode in the electrolytic cell with NiCoMo based i.a. when operated in the temperature range 30–70 °C.

There is a significant decrease of the total resistance of the cathode with increasing the operating temperature observed, at a given overvoltage. This is expected electrocatalytic behavior and is in good agrement with the observations made through polarisation measurements. On the other hand, when increasing the cathodic overvoltage there is evident formation of a second semicircle at high frequency region. The low frequency semicircle is ascribed to the charge transfer process, e.g. Volmer reaction in the HER mechanism, while the high frequency semicircle could be associated with the mass transfer processes of the adsorbed species at the cathode. The origin of these mass transfer processes at the cathode is very complex, due to the complex mechanism of the *in-situ* activation using the NiCoMo based i.a. One of the processes is electrodeposition of the ionic species from the NiCoMo based i.a. on the cathode which occurs simultaneously with the formation of the H_{ads} intermediate (Volmer reaction of the HER mechanism). Co-deposition of the metallic species on the cathode enables increase of the surface roughness, as we have previously reported [11]. The other process that could contribute to the mass transfer effects associated to this high frequency feature is the influence of ethylen–diamine ligands of the Co based complex used[10]. The decomposition of the organic ligands is also influencing the cathode roughness, acting as a surface cleaning agent. The obtained EIS spectra were submitted to fitting procedure in order to obtain contributions of the specific components like electrolyte resistance, charge transfer resistances and double layer capacitances, to the total impedance of the electrolytic cell. The equivalent circuits used are presented in Fig. 4.

The Randles electrical equivalent circuit model, Fig. 4(a), has been mostly used to explain the AC impedance of the HER on nickel-based electrodes in the absence of a response related to the hydrogen adsorption. Armstrong equivalent circuit, Fig. 4(b), is used to describe the AC impedance behavior when the second semicircle appear in the Nyquist plots [18]. In both equivalent circuits, R_e is the electrolyte resistance and R_{ct} represents the charge transfer resistance for the electrode reaction at the working electrode (WE), while C_{dl} denotes the double layer capacitance of the WE, R_p is basically related to the mass transfer resistance of the adsorbed intermediate H_{ads}, usually called pseudo-resistance, and C_p is the pseudo capacitance of the WE. The deviation from the ideal capacitance behavior corresponds to a frequency-dependent phase-angle and the this behavior can be represented by a so-called constant phase element, CPE [19]. This capacitance dispersion of solid electrodes depends strongly on the state of the electrode's surface, e.g. its roughness and degree of polycrystallinity, and also, importantly, on anion adsorption. The double-layer capacitance C_{dl}, of the cathode could be estimated using equation [20–22]:

$$C_{dl} = [T(R_e^{-1} + R_{ct}^{-1})^{-(1-\alpha)}]^{1/\alpha} \quad (7)$$

where T represents the capacitance parameter obtained as the result of fitting (F s^{-1} cm^{-2}), R_{ct} is the charge-transfer resistance (Ω cm^2) and α is independent exponent ($0 < \alpha < 1$).

The EIS parameters of the electrolytic cell obtained via equivalent circuit fitting procedure are presented in Table 2, for 25 °C and a cathodic overpotential of 150 mV.

In the case of standard electrolyte, the Randles equivalent circuit was used for fitting of the experimental EIS data, whereas the

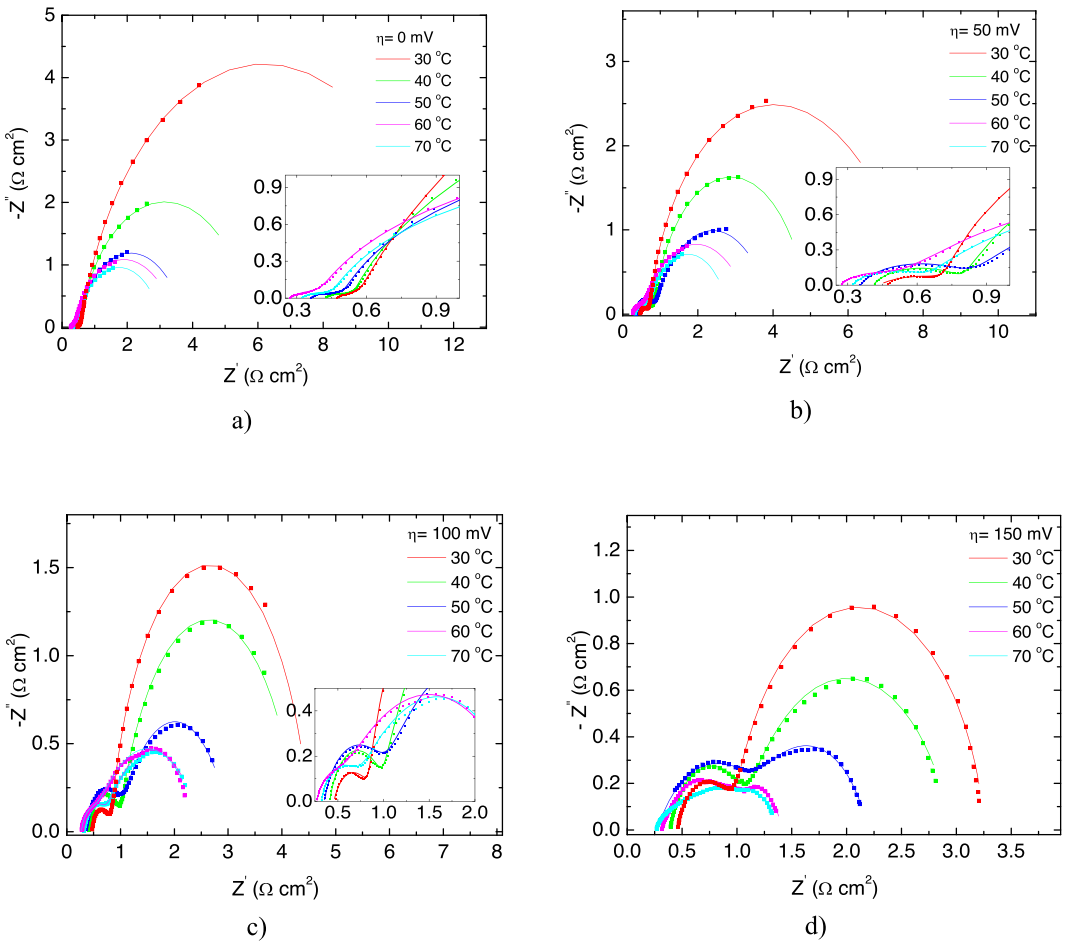

Fig. 3. Nyquist plots for NiCoMo based i.a. (a)–(d) with increasing cathodic overvoltage at temperature range from 30 to 70 °C and different overvoltage; inserts represent high frequency region. Lines were obtained by the fitting procedure using Armstrong equivalent circuit.

Armstrong circuit was used for the *in-situ* activated electrolytic system. Comparison of the parameters obtained at 150 mV cathodic overvoltage and 298 K shows significant decrease of the total resistance of the electrolytic cell. The electrolyte resistance, R_e, does not change very much, and being slightly higher for 6 M KOH + NiCoMo, at room temperature, which could be atributed to the difference in the ionic species mobility and the interaction of Ni, Co and Mo cations with the highly concetrated KOH solution. The main difference is observed in the charge transfer resistance values, which is about 150 times lower in the case when NiCoMo based i.a. was added to 6 M KOH. This significantly decreased R_{ct} values are in good agreement with the exchange current density values, obtained from polarisation measurements. Also, this comparison of the EIS spectra shows that the charge transfer reaction, eg. Volmer reaction, is a RDS in the HER mechanism, at room temperature. The co-deposition of the metallic species on the Ni cathode [11] results in the significant increase of the double layer capacitance via increase of the surface roughness. The surface roughness, σ, could be estimated from EIS data by dividing the C_{dl} values with 20 μF/cm², which is the value of the capacitance for relatively smooth surfaces [22]. Increasing of the operating temperature of the electrolytic cell with NiCoMo based i.a. results in further decrease of the R_{ct} and an increase in C_{dl} values, which is an expected behavior [23], as well in increase of the roughness factor. The increased surface area corresponds to a higher number of active centers available for hydrogen adsorption (Volmer reaction) and other mass transfer processes (simultaneous co-deposition and the ligands effects), which are associated with the pseudo-resistance and pseudo-capacitance values. The R_p values do not change significantly with increasing temperature and overvoltage, and are generally lower than R_{ct} values. The trend of decreasing R_{ct} with increasing overvoltage would eventually result in this high frequency semi-circle to dominate the shape of EIS spectra. This could lead to the conclusion that the Heyrovsky reaction is RDS when the NiCoMo based i.a. was added to 6 M KOH, like it was observed from the polarisation measurements, Fig. 1.

As shown below the data obtained by fitting the experimental EIS spectra, allowed us to differentiate the specific contributions

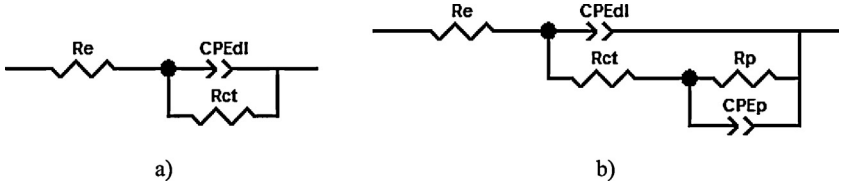

Fig. 4. (a) Randles and (b) Armstrong equivalent circuits used for fitting of the EIS data.

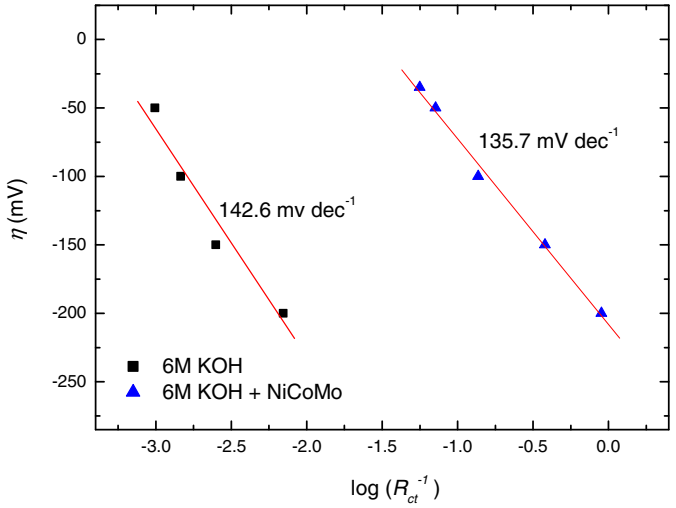

Fig. 5. $\eta - \log(R_{ct})^{-1}$ plots for the HER on Ni in standard electrolyte and 6 M KOH + NiCoMo based i.a., at 298 K, obtained from data taken from the EIS measurements.

of the Volmer reaction and, possibly, Heyrovsky reaction to determining the overall rate of the HER, Fig. 5.

Experimentally obtained polarisation curves for Ni electrode activated with i.a. clearly shows two distinct regions with different values of Tafel slopes corresponding to theoretically presumed Volmer–Heyrovski catalytic mechanism. When Tafel slope has value of ~120 mV dec^{-1}, RDS can be either one of two steps in overall reaction. It was shown in Fig. 5., that the charge transfer reaction is a RDS for the HER at Ni cathode in standard, 6 M KOH electrolyte, giving the slope of 142.6 mV dec, which is very near to the theoretical value of 120 mV dec^{-1} for Volmer reaction. The obtained slope of 135.7 mV dec^{-1} in the case of NiCoMo based i.a. also indicates the Volmer reaction as RDS of the HER. This means that the change in the shape of the polarisation curve at Fig. 1., does not prove the change in the HER mechanism.

The temperature dependence of the kinetic parameters, obtained using polarisation and EIS measurements, is compared in Fig. 6 in the form of Arrhenius plots, for the 6 M KOH + NiCoMo based i.a. electrolyte.

Taking into account the values of the exchange current densities, as a measure of the HER kinetics, and charge transfer resistances, obtained from the EIS spectra, we found a very good between the

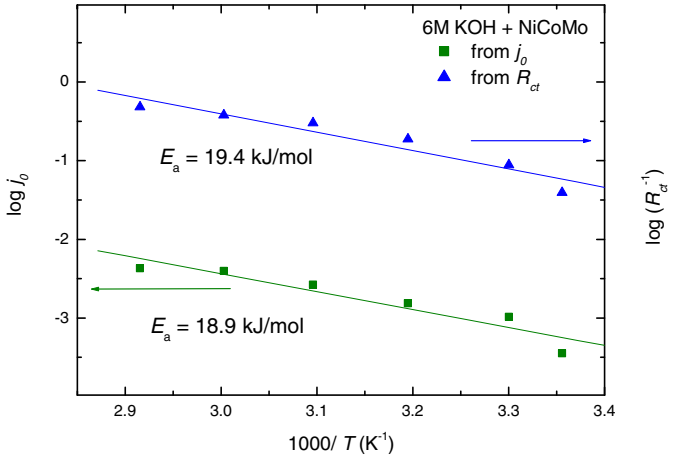

Fig. 6. Dependence on temperature (Arrhenius plots) of the exchange current density for the NiCoMo based i.a.; and of the charge transfer resistance for the NiCoMo based i.a. The lines represent linear fitting results.

activation energy values calculated from the slopes of the corresponding Arrhenius plots (Fig. 6), which were equal to 18.9 kJ/mol and 19.4 kJ/mol, respectively. These values are significantly lower compared to the activation energy of about 40 kJ/mol for the HER at Ni cathode in standard electrolyte [11,23]. This decrease in the activation energy when the NiCoMo based i.a. is added to 6 M KOH is in consistence with the decrease of the energy consumption of the electrolytic cell, reported previously [6,11,24]. Similar activation energies, obtained using different techniques, indicate the Volmer reaction as the RDS for the HER, in the case of *in-situ* activated electrolyte. The overall HER reaction is shown to proceed via Volmer–Heyrovsky pathway, while it is now evident that the Volmer reaction is the RDS. This means that the pseudo-resistance and pseudo-capacitance could not be atributed solely to the hydrogen adsorption (Heyrovsky reaction), but also to the effects corresponding to the mass transfer processes, such as co-deposition of metallic species form i.a. and ligand decomposition. On the other hand, these mass transfer processes, including hydrogen adsorption indicate that the enhanced electrocatalytic activity towards HER, when using NiCoMo based i.a., could be attributed to the increased surface area of the cathode. But the "true" catalytic effect of the combination of three D-metals, used as ionic activators, is evident through the facilitated charge transfer reaction, compared to Ni cathode. Hence, the co-deposition process of Ni, Co and Mo species on the Ni cathode provides a large number of active centres for hydrogen adsorption, with the synergetic effect giving electronic structure suitable for the HER. These observations could not be made just through the Tafel analysis, but in combination with the detailed analysis of the EIS spectra. Again, it is evident that the EIS measurements were of the crucial role in determining the HER mechanism, especially under the conditions of complex *in-situ* activation of the alkaline electrolysis.

4. Conclusions

In this paper, we have investigated the influence of *in-situ* added ionic activators to 6 M KOH for hydrogen production. The polarisation curves in the case of NiCoMo activated electrolyte show the existence of two slopes: 42 mV dec^{-1} at lower potentials and 143 mV dec^{-1} at higher potentials. Further, analysis to determine the RDS was done by means of EIS. The existance of two Tafel slopes could be associated with the relation between the exchange current density and the electronic structure of the composite electrodeposits. EIS measurements were perfomed and it was shown that these measurements were of crucial importance in determining the HER mechanism.The data obtained by fitting the experimental EIS data, allowed us to differentiate the specific contributions of the Volmer reaction and Heyrovsky reaction to the overall rate of the HER mechanism. In determining the HER mechanism by using EIS measurements, the co-deposition process of complex Ni, Co and Mo species on the Ni cathode provided a large number of active centres for hydrogen adsorbtion, with the synergetic effect giving electronic structure suitable for the HER. Since the obtained charge transfer resistance (R_{ct}) has much higher values then all the other resistances taken into account combined, it was concluded that the Volmer reaction is the RDS of the HER. Using obtained values for the exchange current densities and charge transfer resistances, substracted from the EIS spectra, we found a very good agreement in the Arrhenius plots. By adding our NiCoMo based ionic activators to standard electrolyte we achievied activation energy values of 18.9 kJ/mol and 19.4 kJ/mol. These values are significantly lower compared to the activation energy for the HER at Ni cathode in standard electrolyte.

Acknowledgment

The authors gratefully acknowledge financial support of the Ministry of Education, Science and Technological Development of Republic of Serbia through project no. OI172045.

References

[1] J. Ivy, Summary of Electrolytic Hydrogen Production, Milestone Completion Report, US Departmant of Energy, Colorado, 2004.
[2] L.M. Gandı, R. Oroz, A. Ursu, P. Sanchis, P.M. Die, Renewable hydrogen production: performance of an alkaline water electrolyzer working under emulated wind conditions, Energy Fuels 21 (2007) 1699–1706.
[3] I. Ulleberg, Modeling of advanced alkaline electrolyzers: a system simulation approach, Int. J. Hydrogen Energy 28 (2003) 21–33.
[4] W. Kreuter, H. Hofmann, Electrolysis the important energy transformer in a world of sustainable energy, Int. J. Hydrogen Energy 23 (1998) 661–666.
[5] M. Wang, Z. Wang, Z. Guo, Z. Li, The enhanced electrocatalytic activity and stability of NiW films electrodeposited under super gravity field for hydrogen evolution reaction, Int. J. Hydrogen Energy 36 (2011) 3305–3312.
[6] C. Lupi, A. Dell'Era, M. Pasquali, *In-situ*activation with Mo of Ni–Co alloys for hydrogen evolution reaction, Int. J. Hydrogen Energy 39 (2014) 1932–1940.
[7] D.L. Stojić, M.P. Marčeta, S.P. Sovilj, Š.S. Miljanić, Hydrogen generation from water electrolysis—possibilities of energy saving, J. Power Sources 118 (2003) 315–319.
[8] S.G. Neophytides, S. Zafeiratos, G.D. Papakonstantinou, J.M. Jaksic, F.E. Paloukis, M.M. Jaksic, Extended Brewer hypo–hyper-d-interionic bonding theory—I. Theoretical considerations and examples for its experimental confirmation, Int. J. Hydrogen Energy 30 (2005) 113–147.
[9] S.G. Neophytides, S. Zafeiratos, G.D. Papakonstantinou, J.M. Jaksic, F.E. Paloukis, M.M. Jaksic, Extended Brewer hypo-hyper-d-interionic bonding theory II. Strong metal-support interaction grafting of composite electrocatalysts, Int. J. Hydrogen Energy 30 (2005) 393–410.
[10] C. Lacnjevac, M. Jaksic, Synergetic electrocatalytic effect of d-metals on the hydrogen evolution reaction in industrially important electrochemical processes, J. Res. Inst. Catal. Hokkaido Univ. 31 (1983) 7–34.
[11] S.L. Maslovara, M.P. Marceta Kaninski, I.M. Perovic, P.Z. Lausevic, G.S. Tasic, B.B. Radak, et al., Novel ternary Ni–Co–Mo based ionic activator for efficient alkaline water electrolysis, Int. J. Hydrogen Energy 38 (2013) 15928–15933.
[12] G.S. Tasic, S.P. Maslovara, D.L. Zugic, A.D. Maksic, M.P. Marceta Kaninski, Characterization of the Ni–Mo catalyst formed *in-situ*during hydrogen generation from alkaline water electrolysis, Int. J. Hydrogen Energy 36 (2011) 11588–11595.
[13] N. Krstajić, M. Popović, B. Grgur, M. Vojnović, D. Šepa, On the kinetics of the hydrogen evolution reaction on nickel in alkaline solution, J. Electroanal. Chem. 512 (2001) 16–26.
[14] J. Divisek, H. Schmitz, B. Steffen, Electrocatalyst materials for hydrogen evolution, Electrochim. Acta. 39 (1994) 1723–1731.
[15] M. Jaksic, Advances in electrocatalysis for hydrogen evolution in the light of the Brewer–Engel valence-bond theory, Int. J. Hydrogen Energy 12 (1987) 727–752.
[16] N. Krstajic, V. Jovic, B. Gajic-Krstajic Jovic, A. Antozzi, G. Martelli, Electrodeposition of Ni–Mo alloy coatings and their characterization as cathodes for hydrogen evolution in sodium hydroxide solution, Int. J. Hydrogen Energy 33 (2008) 3676–3687.
[17] P.R. Rowland, Electrolytic separation factor of protium and deuterium, Nature 218 (1968) 945–946.
[18] R.D. Armstrong, M. Henderson, Impedance plane display of a reaction with an adsorbed intermediate, J. Electroanal. Chem. Interfacial Electrochem. 39 (1972) 81–90.
[19] E. Barsouko, J. Macdonald, Impedance spectroscopy theory, experiment, and applications, Wiley (2005).
[20] C.H. Hsu, F. Mansfeld, Technical note concerning the conversion of the constant phase element parameter Y0 into a capacitance, Corrosion 57 (2001) 747–748.
[21] V.D. Jović, B.M. Jović, EIS and differential capacitance measurements onto single crystal faces in different solutions, J. Electroanal Chem. 541 (2003) 1–11.
[22] V.D. Jović, B.M. Jović, EIS and differential capacitance measurements onto single crystal faces in different solutions, J. Electroanal Chem. 541 (2003) 13–21.
[23] S.M. Miulovic, S.L. Maslovara, I.M. Perovic, V.M. Nikolic, M.P. Marceta Kaninski, Electrocatalytic activity of ZnCoMo based ionic activators for alkaline hydrogen evolution—Part II, Appl. Catal. A Gen. 451 (2013) 220–226.
[24] T. Yuan, R. Li, K. Zhou, Electrocatalytic properties of Ni–S–Co coating electrode for hydrogen evolution in alkaline medium, Trans. Nonferrous Met. Soc. China 17 (2007) 762–765.